Magneto-transport and magnetization studies of Pr$_{2/3}$Ba$_{1/3}$MnO$_3$:Ag$_2$O composite manganites

Magneto-transport and magnetization studies of $Pr_{2/3}Ba_{1/3}MnO_3$:Ag_2O composite manganites

Neeraj Panwar[1,2]**, D K Pandya**[2] **and S K Agarwal**[1,3]

[1] National Physical Laboratory, Dr K S Krishnan Road, New Delhi-110012, India
[2] Department of Physics, Indian Institute of Technology, New Delhi-110016, India

E-mail: prof.agarwal@gmail.com

Abstract

Magneto-transport and magnetic studies carried out on the $(1 - x)Pr_{2/3}Ba_{1/3}$ $MnO_3 + xAg_2O$ ($x = 0$–30 mol%) composite system are reported here. Two transitions (T_{P1} and T_{P2}) are observed in the electrical resistivity of the pristine $Pr_{2/3}Ba_{1/3}MnO_3$ (PBMO) system. With addition of Ag_2O electrical resistivity decreases. While T_{P1} gets sharper, T_{P2} disappears with increasing Ag_2O content. Electrical resistivity fitting below T_{P2} indicates that PBMO exhibits a crossover from a spin dependent scattering-like polycrystalline material to a single crystalline material in composites. Low temperature resistivity upturn, which results from the combined effect of weak localization, electron–electron and electron–phonon scattering mechanisms, also decreases in the composite materials. The enhanced intrinsic magneto-resistance seen in the composite system has been ascribed to factors like decrease in electrical resistivity due to the formation of metallic Ag from Ag_2O dissociation, disorder reduction, magnetic inhomogeneity and growth of spin clusters. The monotonic decrease in the extrinsic magneto-resistance due to Ag is found to be related to the disappearance of the energy barrier formed at the grain boundary. The observed decrease in the magnetization below the Curie temperature (T_C) is considered vis-à-vis the magnetic volume reduction and the non-magnetic Ag acting as a pinning centre to the domain rotation.

1. Introduction

Mixed valent perovskite manganites have been under intense research after the finding of the colossal change in the electrical resistivity with magnetic field [1, 2]. This so-called colossal magnetoresistive effect (CMR) is related to the double-exchange mechanism and is viewed as an intrinsic property of manganite materials [3]. In single-crystalline film the huge decrease

---

[3] Author to whom any correspondence should be addressed.

in the electrical resistivity under the application of a magnetic field occurs in the vicinity of the Curie temperature (T_C) only. This, in fact, poses a serious problem for the practical utility of such materials. From the application point of view, it is desired that the CMR effect should occur in a broad temperature range and under the application of a low magnetic field [2]. Attempts to improve the electrical and magnetic properties of such materials have led to the observation of another type of magneto-resistance, intergranular or extrinsic magneto-resistance, related to the spin polarized tunnelling or spin dependent scattering of the charge carriers at the grain boundaries in polycrystalline or fine particle systems [4, 5]. It was reported that the large MR value lies in the complete spin polarization of the material. In order to get clear knowledge of MR due to the grain boundary effects researchers have synthesized composite systems with some additives. This has been achieved by making the grain boundary insulating (thus creating a barrier in the way of the charge carriers) [6–11] or by making it conducting [12–17]. Besides this, hard and soft magnetic materials have also been added to the parent perovskite manganites [18, 19]. The results for the electrical, magnetic and thermal properties have been quite interesting and different from those of the pristine sample. But the composite of a manganite material with an insulating additive results in the increase of electrical resistivity (though it increases MR) and a decrease in the I–M transition to lower temperatures that hampers any practical utility of these materials. Such a problem of increase in resistivity can be sorted out if manganite composites with appropriate metallic additives are synthesized. Addition of Ag through Ag_2O, $AgNO_3$ etc has revealed drastic changes in the composite material properties [13–17]. The scenario bears similarity to high-temperature superconductors where enhanced grain boundary properties like the improvement in the critical current density and in the conduction noise are observed with Ag addition [20]. Recently, it has been shown that Ag addition has resulted in a high magneto-resistance value at room temperature in a sol–gel synthesized LaBaCaMnO system [13]. Silver, therefore seems to be a good choice as an additive in manganites also. Though there exist several reports of Ag composites with manganites that show a single insulator–metal (I–M) transition in the electrical resistivity, no study so far seems to have been carried out on a composite of Ag with manganite that exhibits two transitions in the electrical resistivity. $Pr_{2/3}Ba_{1/3}MnO_3$ (PBMO) is one such material that shows two I–M transitions (T_{P1} and T_{P2}) and Ag addition is expected to generate results that are different from those for composite manganites with a single I–M transition. The higher temperature transition (T_{P1}) in PBMO is due to the competition between the double-exchange and super-exchange mechanisms inside the grain and the lower temperature broad transition (T_{P2}) arises from the large grain boundary effects [21]. The manganite PBMO is also interesting because it does not follow the average ionic size $\langle r_A \rangle$ versus T_C criteria proposed by Hwang *et al* [22].

2. Experimental details

A polycrystalline composite system $(1 - x)$PBMO $+ x$Ag$_2$O (where $x = 0$, 10, 20, 27, 30 mol%) was synthesized using the conventional solid-state reaction method. Firstly polycrystalline PBMO powder was obtained by several calcinations (with intermediate grindings) and final sintering was done at 1260 °C for 25 h. Ag_2O was then mixed with calcined PBMO powder in the desired molar ratios and the ground mixture was treated at 1260 °C for 100 min. To ascertain the phase purity, x-ray diffractograms of the samples were recorded using a Philips machine (Cu Kα, $\lambda = 1.54$ Å). Scanning electron micrographs (SEM) were recorded using a LEO SEM 440 machine [equipped for energy dispersive spectroscopy (EDAX)] operating at 20 kV. Electrical resistivity with and without a magnetic field (5 T) was recorded using the conventional four-probe method from 300 to 10 K. The magnetic field was
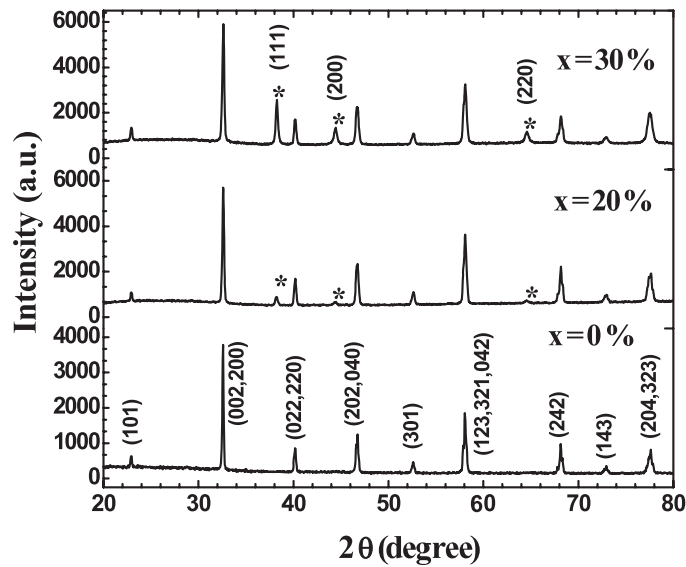
Figure 1. X-ray diffractograms of 0, 20 and 30 mol% Ag_2O added PBMO composites. * represents Ag peaks.

applied parallel to the current direction. The magneto-resistance has been defined as

$$MR(\%) = [(\rho_0 - \rho_H)/\rho_0] * 100,$$

where ρ_H and ρ_0 are the electrical resistivities with and without a magnetic field, respectively. The variation of magnetization (at 0.5 T) with temperature (300–10 K) in the zero field configuration (ZFC) was recorded on a PPMS (Quantum Design, model 6000) system.

3. Results and discussion

Figure 1 shows the x-ray diffractograms of the $(1 - x)$PBMO $+ x$Ag$_2$O system. It is clear that Ag$_2$O because of its low dissociation temperature (300 °C) gets converted into metallic Ag. Peaks of cubic Ag are clearly depicted in the diffractograms of the composites (represented by *). Though attempts have been made to substitute Ag at the rare-earth site in manganites [23, 24], transmission electron microscopy (TEM) and electron energy loss spectroscopy (EELS) results carried out have shown that Ag cannot be substituted at the rare-earth site which segregates at the grain surface/boundary [25]. As there is a large difference [26] between the ionic size of Ag (I.R.^{VI} = 1.15 Å) and the Mn ion (Mn^{3+}, I.R.^{VI} = 0.645 Å; Mn^{4+}, I.R.^{VI} = 0.53 Å), Hume-Rothery criteria for ion substitution are also not satisfied. It is therefore concluded that Ag remains at the grain boundary thereby making the composite a two-phase material. The parent compound PBMO, however, is a single-phase material with orthorhombic structure. Figure 2(a) shows the scanning electron micrograph of the pristine PBMO sample. EDAX measurement confirmed the nominal composition and absence of any other phase. However, for 30% Ag$_2$O added PBMO (figure 2(b)) it is clear that Ag is in the form of thin layers (bright region) at the grain boundary (confirmed through EDAX). The connectivity among the PBMO grains seems enhanced with Ag. Figure 3 shows the variation in electrical resistivity with temperature of the composite system. The parent material PBMO shows two I–M transitions in the electrical resistivity with T_{P1} at 194 K and T_{P2} at 160 K.
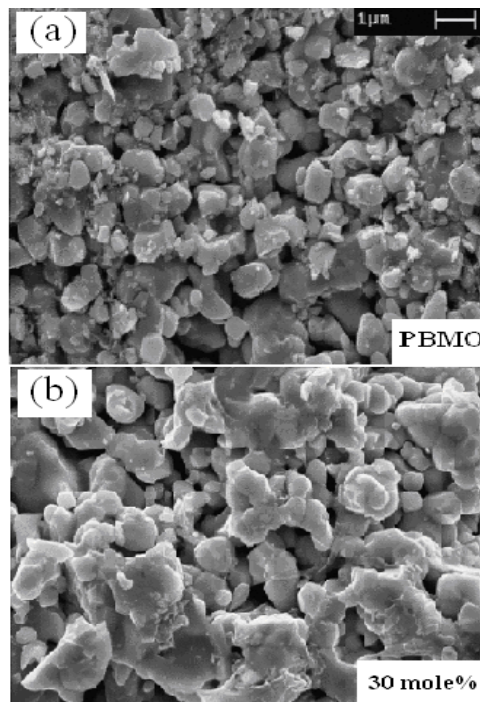
Figure 2. Scanning electron micrographs for PBMO composites with (a) $x = 0$ and (b) for $x = 30$ mol% Ag_2O.

T_{P1} results from the competition between double-exchange and super-exchange mechanisms inside the grain whereas T_{P2} arises due to grain boundary effects ensuing from the ionic size mismatch between Pr^{3+} (I.R.^{IX} = 1.179 Å) and Ba^{2+} (I.R.^{IX} = 1.47 Å) present at the rare-earth site. This large ionic size mismatch creates a strain in the lattice, which the lattice is unable to sustain and hence unloads it to the grain boundary. The transferred strain at the grain boundary tilts the MnO_6 octahedra there and thus the electron transfer probability gets weakened and the transition due to the grain boundary separates out from the grain [21]. The results on PBMO are consistent with other Ba-based manganite systems like NdBaMnO and LaBaMnO [27, 28]. While T_{P1} remains almost unchanged, electrical resistivity decreases with Ag in all the composite samples up to 30 mol% Ag_2O. In some reports a decrease of electrical resistivity has been noticed only up to 27% Ag_2O and increasing thereafter [13, 15]. It is conjectured that in the present system Ag is probably more tightly bound and does not volatilize even up to 30 mol%. Similarly the rate of decrease of electrical resistivity at T_{P2} is much faster in our case as only one sharp transition is obtained for 25 mol% Ag_2O (inset of figure 3) beyond which T_{P2} disappears. The development of a second I–M like transition has been reported in some manganite composites with 25 mol% Ag_2O [15, 16] but such a phenomenon has not been observed here. The observed decrease in resistivity with Ag_2O addition can be attributed to the following two factors [15]. Firstly, oxygen liberated from the breaking of Ag–O bonds is likely to move inside the grains, compensating for the oxygen loss there, if any, by filling the vacancy in the bond between Mn^{3+} and Mn^{4+}. This would help ease the electron transfer in the double-exchange mechanism, resulting in the decrease of electrical resistivity. Secondly, the presence of Ag in the grain boundary (GB) regions would also render the GBs more conducting, by opening the new conducting channels among the
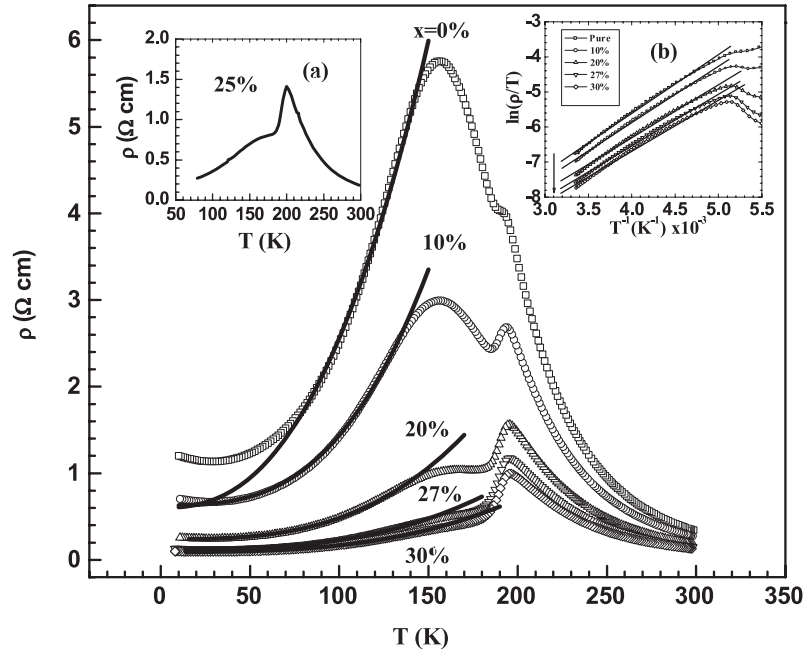
Figure 3. $\rho(T)$ of the different composite systems. Solid lines represent the fitting of $\rho(T)$ below T_{P2} with equation (5). Inset (a) refers to $\rho(T)$ for 25 mol% Ag$_2$O added PBMO and inset (b) shows the fitting of $\rho(T)$ above T_{P1} with equation (3).

PBMO grains. The barrier formed by the disorder/strain at the grain boundary decreases or rather disappears with higher concentrations of Ag$_2$O. T_{P1}, however, remains almost unchanged owing to a fixed Mn^{3+}/Mn^{4+} ratio. Therefore, pristine material PBMO having the magnetic–insulator–magnetic structure turns into a magnetic–metal–magnetic structure material with Ag$_2$O addition. Another important phenomenon observed here is the re-entrant insulating behaviour at lower temperatures (figure 4). In the case of intergranular tunnelling in polycrystalline manganites, application of a higher magnetic field shifts the resistivity upturn temperature T_{min} to lower temperatures as well as flattening the re-entrant behaviour [29]. However, in the present case, T_{min} shifts slightly to higher temperature and the upturn also does not disappear with applied magnetic field (inset of figure 4). This rules out intergranular tunnelling as a possible cause of the resistivity minimum in this class of manganites. The other possible explanation for the resistivity upturn could be the Kondo effect [30], where the magnetic moment scattering due to a small number of magnetic ions in a non-magnetic matrix causes the resistivity upturn. However, this effect does not hold good here as all the samples under consideration are ferromagnetic. We then tried to fit the resistivity data ($T < 50$ K) using the equation

$$\rho(T) = \{1/(a + bT^{1/2})\} + \rho_2 T^2 + \rho_5 T^5, \tag{1}$$

where the term in the parentheses arises due to the weak localization effect [31], 'a' is temperature independent residual conductivity and 'b' is the diffusion constant. The other two terms, namely $\rho_2 T^2$ and $\rho_5 T^5$, arise due to the electron–electron and electron–phonon scattering, respectively [32]. However, we can expand equation (1) binomially as

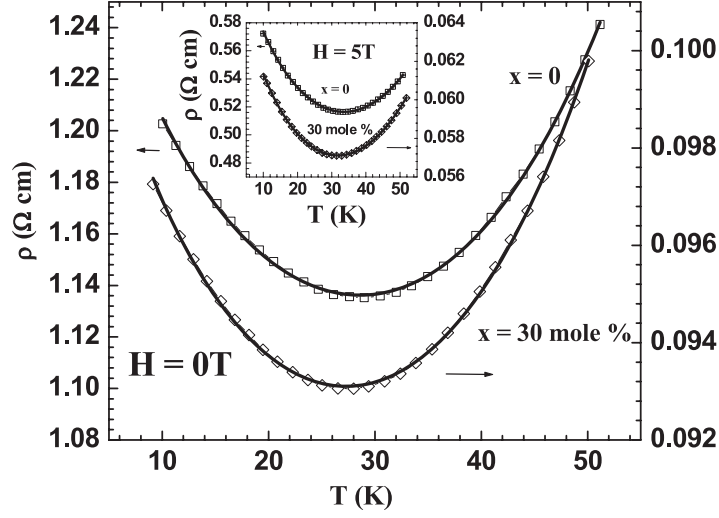$$\rho(T) = \rho_0 - \rho_1 T^{1/2} + \rho_2 T^2 + \rho_5 T^5, \tag{2}$$

Figure 4. Low temperature electrical resistivity fitting in PBMO and for 30 mol% composite using equation (2). Inset shows fitting of data under 5 T magnetic field.

Table 1. Low temperature resistivity fitting (<50 K) (equation (2)).

x (mol%)	ρ_0 (Ω cm)	ρ_1 (Ω cm K$^{-1/2}$)	ρ_2 (Ω cm K^2)	ρ_5 (Ω cm K^5)
0	1.40 ± 0.0036	0.065 ± 0.0011	$0.001 \pm 2.7 \times 10^{-6}$	$(1.4 \pm 0.1) \times 10^{-10}$
10	0.816 ± 0.0017	0.036 ± 0.0005	$(5 \pm 0.13) \times 10^{-5}$	$(8.3 \pm 0.5) \times 10^{-11}$
20	0.294 ± 0.0006	0.012 ± 0.0002	$(2 \pm 0.05) \times 10^{-5}$	$(2.8 \pm 0.2) \times 10^{-11}$
27	0.146 ± 0.0003	0.0056 ± 0.0008	$(9.1 \pm 0.2) \times 10^{-6}$	$(1.1 \pm 0.7) \times 10^{-11}$
30	0.1089 ± 0.0002	0.004 ± 0.0005	$(6.49 \pm 0.14) \times 10^{-6}$	$(8.6 \pm 0.6) \times 10^{-12}$

where $\rho_0 = 1/a$ and $\rho_1 = b/a^2$ are constants. The fitting parameters of the composite systems are shown in table 1. It is observed that the value of the fitting parameters ρ_0, ρ_1, ρ_2, ρ_5 decreases in the composite system. This indicates that the weak localization, electron–electron (e–e) and electron–phonon (e–ph) scattering decrease with Ag, disorder decreases and the material becomes ordered.

The electrical resistivity data above T_{P1} of the composite systems was fitted using the small polaron hopping model [33], the mathematical expression for which is given as

$$\rho = \rho_0 T \exp(E_A/k_B T), \tag{3}$$

where $\rho_0 = [k_B/\upsilon_{ph} N e^2 R^2 C(1 - C) \exp(2\alpha R)]$, k_B is the Boltzmann constant, N is the number of sites per unit volume, R is the intersite spacing, C is the fraction of sites occupied by polarons, α is the wavefunction decay constant, υ_{ph} is the optical phonon frequency and E_A is the activation energy. The calculated activation energy decreases with increasing Ag content, which again confirms that metallic Ag enhances the grain connectivity (table 2). Thus with Ag$_2$O addition the properties of PBMO resemble those of single-crystalline-like material because the barrier height decreases with the activation energy and the spin dependent process gets converted into a normal ferromagnetic metal-like hopping process. This is clearly evident from the MR versus H curve taken at 77 K (figure 5) where a sharp increase occurs in MR for the pure sample PBMO at lower magnetic field values and is followed by a gradual increase at higher H values. These results are similar to those reported by Gupta *et al* [5] for thin films.
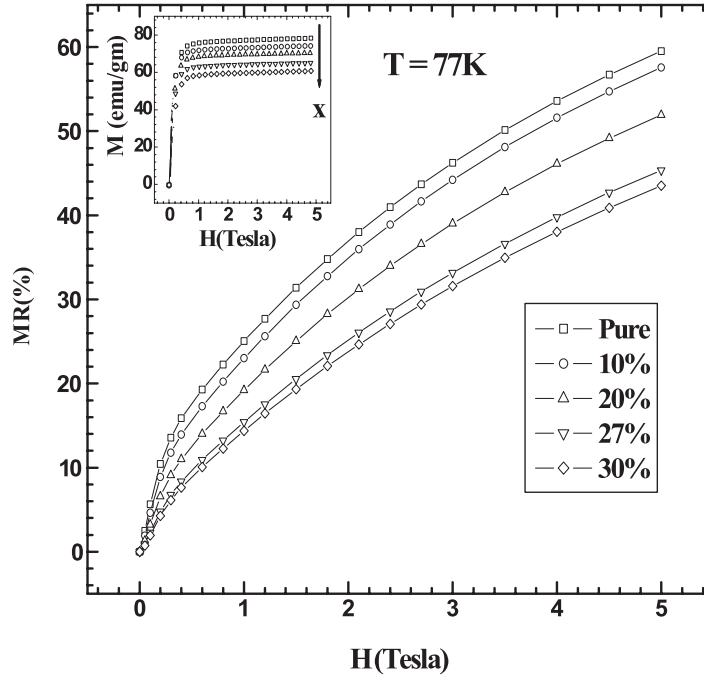
Figure 5. MR variation with magnetic field at 77 K of the composite system. Inset shows the magnetization versus H at the same temperature.

Table 2. Values of activation energy and average spin moment of spin clusters (equation (4)).

	x (mol%)				
	0	10	20	27	30
E_A (meV)	142.85	138.64	130.23	127.31	125.55
$J(\hbar)$	114	159	236	294	317

MR behaviour then changes just like for epitaxial/single-crystalline film on increasing Ag content in PBMO. To further consolidate our idea we varied the magnetization with magnetic field at a fixed temperature of 77 K (inset of figure 5). It is observed that the magnetization at higher magnetic field values decreases with increasing Ag content, which we relate to the increase in the grain size with Ag. Grain growth is also noticed here through the grain size evaluation from the x-ray diffraction peaks, and is in accord with the reported behaviour [17]. The sudden increase in MR at lower magnetic field values is attributed to the domain/grain rotation in the direction of field that decreases the spin dependent scattering at the grain boundary giving a large MR. However, the intrinsic MR gets enhanced and it changes from 62% for a pure sample to 82% for 30 mol% Ag_2O whereas extrinsic MR due to the grain boundary effect gets suppressed (figure 6). Such a behaviour can be understood by invoking the crossover from spin dependent scattering-like polycrystalline to a single-crystalline-like manganite with Ag_2O addition in the pristine PBMO. Figure 6 also indicates that extrinsic MR ($\sim T_{P2}$) in PBMO is more prominent than the intrinsic MR ($\sim T_{P1}$). When a spin polarized electron approaches the grain boundary it suffers a spin dependent scattering (due to a chaotic spin structure), resulting in larger resistivity and a lower T_P value compared to the corresponding values for the grains.
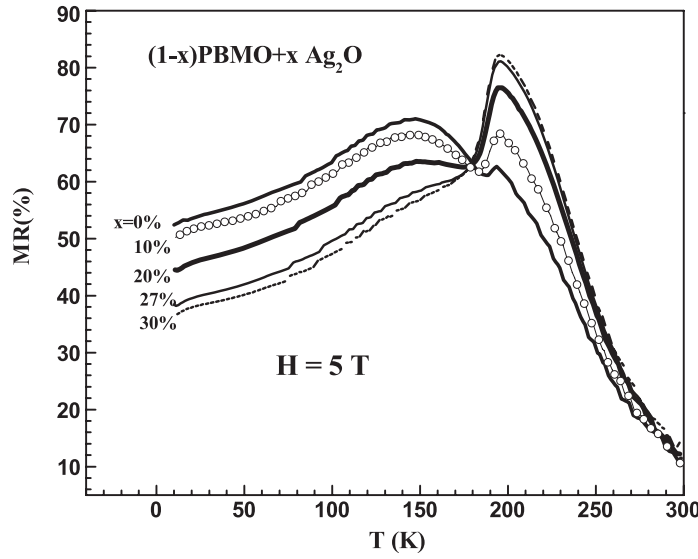
Figure 6. MR versus T of the PBMO + Ag$_2$O composites.

Therefore the resistivity of PBMO is the convolution of these two values. With an applied magnetic field, the relative change in the grain resistivity is small (due to parallel spins) and hence small MR [$\alpha(\rho_0 - \rho_H)$]. However, at the grain boundaries the misaligned spins get aligned, leading to a large change in the grain boundary resistivity and hence large MR. With Ag, the connectivity among the grains increases which makes it behave like single-crystalline material with enhanced conductivity, leading to large MR [$\alpha(1/\rho_0)$] at T_{P1}. This also implies a decrease of the grain boundary density, spin dependent scattering and consequently a decrease of MR around T_{P2}. To further elucidate the MR trend of the composite system we have fitted the MR versus H curve at 190 K (figure 7) by using the Brillouin function (B_J) proposed by Wagner *et al* [34] where MR is proportional to the B_J in the FM region, i.e.

$$\text{MR}(\%) = \{(\rho_0 - \rho_H)/\rho_0\} * 100 = \{A(T)/\rho_0\} * B_J[g\mu_B J(T)/k_B T], \qquad (4)$$

where g is the gyromagnetic ratio, μ_B is the Bohr magneton, $J(T)$ is the average spin moment of the spin clusters that is related to the size of the spin clusters and $A(T)$ is the temperature dependent CMR amplitude which is related to the population of the spin clusters in the ferromagnetic phase. The fitting is shown in figure 7 and it is observed that the size of the spin clusters increases in the composites as the value of $J(T)$ increases (table 2). It is worth mentioning here that this model has been used to explain the MR results in the intrinsic region, i.e. around T_{P1} [12, 15]. However, MR at 77 K is extrinsic in nature (i.e. due to grain boundary effects) even though the composite system behaviour is intrinsic-like due to Ag addition. This leads to a reduction in the MR value at 77 K in the composites. The MR versus H data at 77 K lead to a poor fitting with equation (4), showing the inapplicability of the model in this region. This only implies that the composite system has not fully acquired the status of being completely single-crystalline nature.

The data below T_{P2} are found to obey the following equation

$$\rho = \rho_0 + \rho_n T^n, \qquad (5)$$

where ρ_0 is the electrical resistivity arising from the temperature independent factors like domain walls, grain boundaries, vacancies etc. The term $\rho_n T^n$ depends upon the value of n
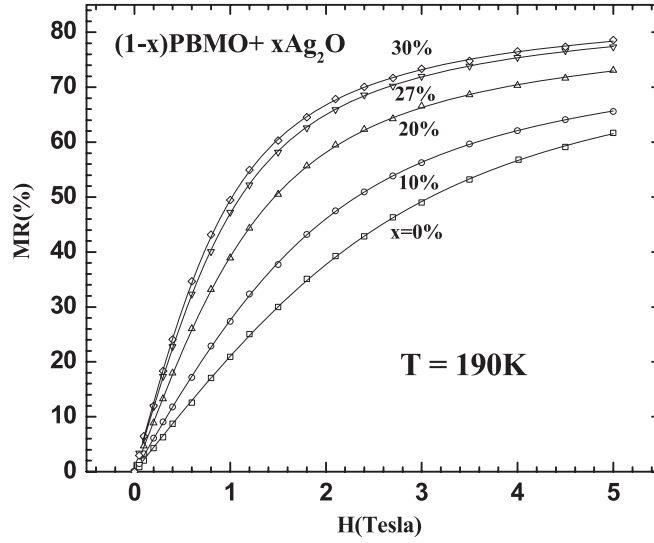
8

Figure 7. MR variation with magnetic field at 190 K. Solid lines represent the theoretical fitting with equation (4).

and can be thought of as arising from electron–electron scattering for $n = 2$, electron–magnon scattering for $n = 2.5$ etc [2]. It is seen that the pristine sample PBMO follows the one-magnon scattering law for $n = 2.5$ and in the composites an unconventional one-magnon scattering law for $n = 3$ is obeyed. It is found that with Ag the low-temperature metallic phase changes from the one-magnon scattering process to an unconventional scattering process (which is followed by the single-crystalline manganite perovskite materials). This is just opposite to what was reported earlier with Ag added to $L_{0.67}Ba_{0.33}Mn_{0.88}Cr_{0.12}O_3$ prepared by the sol–gel method [14], where at low Ag content an unconventional electron–magnon process ($n = 3$) and for higher Ag addition a normal electron–magnon process ($n = 2.5$) were found to be followed. Thus the behaviour of PBMO changes from that of a polycrystalline material to that of a single-crystalline-like material with increasing Ag content. Figure 8 shows the variation of magnetization with temperature of the composite system in the zero field-cooled configuration with 0.5 T field applied on warming. All the samples show a paramagnetic to ferromagnetic transition (T_C). The transition temperature has been deduced from the minimum of dM/dT. The pristine sample shows transition at 194 K which remains practically unchanged with Ag_2O addition, indicating a fixed Mn^{4+} value. However, below T_C the magnetization decreases monotonically with Ag addition. This is similar to an earlier published report [14] and contrary to [17] where it is found to increase with Ag addition in LCMO material. A possible reason for the observed decrease in the M value could be the decrease in the magnetic volume fraction, as Ag is non-magnetic in nature. Besides, as Ag is non-magnetic it can act like a pinning centre for the domain rotation resulting in the decrease in magnetization. The magnetization data below T_C were fitted with the following equation [35, 36]

$$M(T) = M(0) - BT^{3/2} - CT^{5/2}, \qquad (6)$$

where $M(0)$ is the magnetization at 0 K and $B = 0.0587g\mu_B(k_B/D)^{3/2}$ and C are constants. The value of B increases with Ag (1.1076×10^{-6} for pure PBMO to 1.5438×10^{-6} emu $K^{-3/2}$ for 30% Ag_2O) which implies that the stiffness coefficient D will decrease and consequently the strength of the magnetic coupling decreases in the ferromagnetic clusters. It is also clear
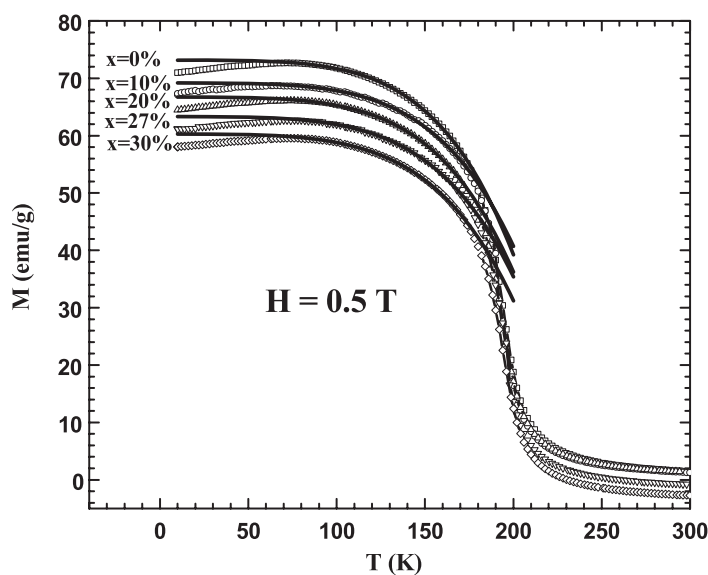
Figure 8. Magnetization variation with temperature of the PBMO + Ag$_2$O composite system (symbols). Solid lines represent the theoretical fitting with equation (6).

that at lower temperatures the theoretical fitting deviates from the experimental results. This may be attributed to the demagnetization factor arising from the sample dimensions.

4. Conclusions

Two transitions (T_{P1} and T_{P2}) are observed in the electrical resistivity of the Pr$_{2/3}$Ba$_{1/3}$MnO$_3$ (PBMO) system. The electrical resistivity decreases with Ag$_2$O addition and its fitting below T_{P2} indicates that PBMO exhibits a changeover from a spin dependent scattering-like polycrystalline material to a single-crystalline-like material. Both T_{P1} and T_C remain almost unchanged, whereas T_{P2} disappears in the composite system with increasing Ag$_2$O content. Low temperature ($<$50 K) resistivity upturn also decreases in the composites. The observed enhanced intrinsic magneto-resistance in the composite system has been viewed in the light of decrease in electrical resistivity due to the formation of metallic Ag, disorder reduction, magnetic inhomogeneity and the growth of spin clusters. The extrinsic magneto-resistance decreases monotonically, which is found to be related to the disappearance of the energy barrier formed at the grain boundary. The decrease in magnetization below T_C is considered in terms of the magnetic volume reduction and metallic Ag acting as a pinning centre for the domain rotation.

Acknowledgments

References

[1] Jin S and Tiefel T H 1994 *Science* **264** 413
[2] Rao C N R and Raveau B (ed) 1998 *Colossal Magnetoresistance, Charge Ordering and Related Properties of Manganese Oxides* (Singapore: World Scientific)
[3] Zener C 1951 *Phys. Rev.* **81** 440
[4] Hwang H Y, Cheong S-W, Ong N P and Batlogg B 1996 *Phys. Rev. Lett.* **77** 2041
[5] Gupta A, Gong G Q, Xiao G, Duncombe P R, Lecoeur P, Trouilloud P, Wang Y Y, Dravid V P and Sun J Z 1996 *Phys. Rev.* B **54** 15629
[6] Moshnyaga V, Damaschke B, Shapoval O, Belenchuk A, Faupel J, Lebedev O I, Verbeeck J, Tendeloo G V, Mücksch M, Tsurkan V, Tidecks R and Samwer K 2003 *Nat. Mater.* **2** 247
[7] Xia Z C, Yuan S L, Zhang G H, Zhang L J, Tang J, Feng W, Liu J, Peng G, Liu L, Li Z Y, Zheng Q H, Cheng L, Tang C Q, Liu S and Xiong C S 2003 *J. Phys. D: Appl. Phys.* **36** 217
[8] Yan L, Kong L B, Yang T, Goh W C, Tan C Y, Ong C K, Rahman M A, Osipowicz T and Ren M Q 2004 *J. Appl. Phys.* **96** 1568
[9] Karmakar S, Taran S, Chaudhuri B K, Sakata H, Sun C P, Huang C L and Yang H D 2005 *J. Phys. D: Appl. Phys.* **38** 3757
[10] Zhang N and Wang M 2006 *Appl. Phys. Lett.* **88** 122111
[11] Yao L D, Zhang W, Zhang J S, Yang H, Li F Y, Liu Z X, Jin C Q and Yu R C 2007 *J. Appl. Phys.* **101** 063905
[12] Yuan X-B, Liu Y-H, Wang C-J and Mei L-M 2006 *Appl. Phys. Lett.* **88** 042508
[13] Yuan X-B, Liu Y-H, Wang C-J and Mei L-M 2005 *J. Phys. D: Appl. Phys.* **38** 3360
[14] Yuan X-B, Liu Y-H, Yin N, Wang C-J and Mei L-M 2006 *J. Magn. Magn. Mater.* **306** 167
[15] Yuan X-B, Liu Y-H, Huang B X, Wang C-J and Mei L-M 2005 *J. Phys. D: Appl. Phys.* **38** 1
[16] Huang Y-H, Yan C-H, Luo F, Song W, Wang Z-M and Liao C-S 2002 *Appl. Phys. Lett.* **81** 76
[17] Awana V P S, Tripathi R, Balamurugan S, Kishan H and Muromachi E T 2006 *Solid State Commun.* **140** 410
[18] Huang Q, Li J, Huang X J, Ong C K and Gao X S 2001 *J. Appl. Phys.* **90** 2924
[19] Yan C-H, Xu Z-G, Zhu T, Wang Z-M, Cheng F-X, Huang Y-X and Liao C-S 2000 *J. Appl. Phys.* **87** 5588
[20] Cohen D, Sorrell C C, Dou S X and Apperley M 1991 *J. Am. Ceram. Soc.* **74** 1541
[21] Panwar N, Sen V, Pandya D K and Agarwal S K 2007 *Mater. Lett.* **61** 4879
[22] Hwang H Y, Cheong S-W, Radaelli P G, Marezio M and Batlogg B 1995 *Phys. Rev. Lett.* **75** 914
[23] Tang T, Cao Q Q, Gu K M, Xu H Y, Zhang S Y and Du Y W 2000 *Appl. Phys. Lett.* **77** 723
[24] Pi L, Hervieu M, Maignan A, Martin C and Raveau B 2003 *Solid State Commun.* **126** 229
[25] Xu Q Y, Wang R P and Zhang Z 2005 *Phys. Rev.* B **71** 092401
[26] Shannon R D 1976 *Acta Crystallogr.* A **32** 751
[27] Barnabe A, Millange F, Maigan A, Hervieu M, Raveau B, Tendeloo G V and Laffez P 1998 *Chem. Mater.* **10** 252
[28] Ju H L, Gopalakrishnan J, Peng J L, Li Q, Xiong G C, Venkatesan T and Greene R L 1995 *Phys. Rev.* B **51** 6143
[29] Auslender M, Karkin A E, Rosenberg E and Gorodetsky G 2001 *J. Appl. Phys.* **89** 6639
[30] Kondo J 1964 *Prog. Theor. Phys.* **32** 37
[31] Lee P A and Ramakrishnan T V 1985 *Rev. Mod. Phys.* **57** 287
[32] Ziman J M 1967 *Electrons and Phonons* (Oxford: Oxford University Press)
[33] Mott N F and Davis E A (ed) 1971 *Electronic Process in Noncrystalline Materials* (Oxford: Clarendon)
[34] Wagner P, Gordon I, Trappeniers L, Vanacken J, Herlach F, Moshchalkov V V and Bruynseraede Y 1998 *Phys. Rev. Lett.* **81** 3980
[35] Jaime M, Lin P, Salamon M B and Han P D 1998 *Phys. Rev.* B **58** 5901
[36] Fernandez-Baca J A, Dai P, Kawano-Furukawa H, Yoshizawa H, Plummer E W, Katano S, Tomioka Y and Tokura Y 2002 *Phys. Rev.* B **66** 054434